Overall Kinetic Mechanism of Saccharopine Dehydrogenase (L-Glutamate Forming) from *Saccharomyces cerevisiae*[†]

Ashwani Kumar Vashishtha, Ann H. West, and Paul F. Cook*

Department of Chemistry and Biochemistry, University of Oklahoma, 620 Parrington Oval, Norman, Oklahoma 73019

Received January 16, 2008; Revised Manuscript Received March 20, 2008

ABSTRACT: Kinetic studies were carried out for histidine-tagged saccharopine reductase from *Saccharomyces cerevisiae* at pH 7.0, suggesting a sequential mechanism with ordered addition of reduced nicotinamide adenine dinucleotide phosphate (NADPH) to the free enzyme followed by L-α-aminoadipate-δ-semialdehyde (L-AASA) which adds in rapid equilibrium prior to L-glutamate in the forward reaction direction. In the reverse reaction direction, nicotinamide adenine dinucleotide phosphate (NADP) adds to the enzyme followed by addition of saccharopine. Product inhibition by NADP is competitive vs NADPH and noncompetitive vs α-AASA and L-glutamate, suggesting that the dinucleotide adds to the free enzyme prior to the aldehyde. Saccharopine is noncompetitive vs NADPH, α-AASA, and L-glutamate. In the direction of saccharopine oxidation, NADPH is competitive vs NADP and noncompetitive vs saccharopine, L-glutamate is noncompetitive vs both NADP and saccharopine, while L-AASA is noncompetitive vs saccharopine and uncompetitive vs NADP. The sequential mechanism is also corroborated by dead-end inhibition studies using analogues of AASA, L-glutamate, and saccharopine. 2-Amino-6-heptenoic acid was chosen as a dead-end analogue of L-AASA and is competitive vs AASA, uncompetitive vs NADPH, and noncompetitive vs L-glutamate. α-Ketoglutarate (α-Kg) serves as the dead-end analogue of L-glutamate and is competitive vs L-glutamate and uncompetitive vs L-AASA and NADPH. In the direction of saccharopine oxidation, *N*-oxalylglycine, L-pipecolic acid, L-leucine, α-ketoglutarate, glyoxylic acid, and L-ornithine were used as dead-end analogues of saccharopine and showed competitive inhibition vs saccharopine and uncompetitive inhibition vs NADP. The equilibrium constant for the reaction was measured at pH 7.0 by monitoring the change in absorbance of NADPH and is 200 M^{-1}. The value is in good agreement with the value determined using the Haldane relationship.

The biosynthesis of L-lysine occurs via the α-aminoadipate (AAA)[1] pathway in euglenoids and higher fungi such as basidiomycetes (*1*). The α-aminoadipate pathway is a member of the glutamate family of amino acid biosynthetic pathways (*2*). The AAA pathway has been reported in *Saccharomyces cerevisiae* (*3*), *Schizosaccharomyces pombe* (*4*), *Penicillium chrysogenum* (*5*), *Neurospora crassa* (*6*), *Magnoporthe grisea*, which is a plant pathogen (*7*), and human pathogenic fungi including *Candida albicans* (*8*), *Aspergillus fumigatus* (*9*), and *Cryptococcus neoformans* (*8*).

Saccharopine reductase (SR) [saccharopine dehydrogenase (L-glutamate forming), EC 1.5.1.10] catalyzes the condensation of L-α-aminoadipate δ-semialdehyde with L-glutamate to give an imine, which is reduced by NADPH to give saccharopine (*7*).

Crystal structures of saccharopine reductase from *S. cerevisiae* and *M. grisea* have been reported (*7, 10*). Structures of the *M. grisea* apo form and ternary, E−NADPH −saccharopine, complex of SR were solved to 2.0 and 2.1 Å, respectively. The enzyme is a homodimer with a molecular weight of ∼50000 and contains one binding site for substrates per subunit. The amino acid sequence of SR is highly conserved in *C. albicans*, *A. fumigatus*, *C. neoformans*, and *S. cerevisiae*, and thus, SR is a potential target for antifungals. In preparation for the development of mechanism-based inhibitors, the kinetic and chemical mechanisms of the enzyme must be known. The pH optimum of SR from *S. cerevisiae* in the direction of saccharopine formation is 7.0 (*11*), while it is 9.5−9.75 in the direction of semialdehyde formation (*11, 12*). Apparent K_m values for L-saccharopine, NADP, and NAD are 2.32 mM, 22 μM, and 54 μM, respectively (*11*), with NADPH a better substrate than NADH in the physiologic reaction direction (*12*).

Thus far, no information is available on the kinetic mechanism of SR. In this paper, we present a detailed steady-state kinetic analysis of the saccharopine reductase reaction in both reaction directions. On the basis of initial velocity studies in the absence and presence of product and dead-end inhibitors, an ordered kinetic mechanism is proposed

[†] This work was supported by the Grayce B. Kerr Endowment to the University of Oklahoma (to P.F.C.), and a grant (GM 071417) from the National Institutes of Health (to P.F.C. and A.H.W.).

* Corresponding author. E-mail: pcook@ou.edu. Tel: 405-325-4581. Fax: 405-325-7182.

[1] Abbreviations: AAA, α-aminoadipate pathway; SR, saccharopine reductase; NADP, nicotinamide adenine dinucleotide phosphate (the + charge is omitted for convenience); NADPH, nicotinamide adenine dinucleotide phosphate (reduced form); OG, oxalylglycine; OAA, oxaloacetate; α-Kg, α-ketoglutarate; HEPES, 4-(2-hydroxyethyl)-1-piperazineethanesulfonic acid; C, competitive; UC, uncompetitive; NC, noncompetitive; IPTG, isopropyl β-D-1-thiogalactopyranoside; LB, Luria−Bertani; Amp, ampicillin; SEM, standard error of the mean.

10.1021/bi800086g CCC: $40.75 © 2008 American Chemical Society
Published on Web 04/17/2008

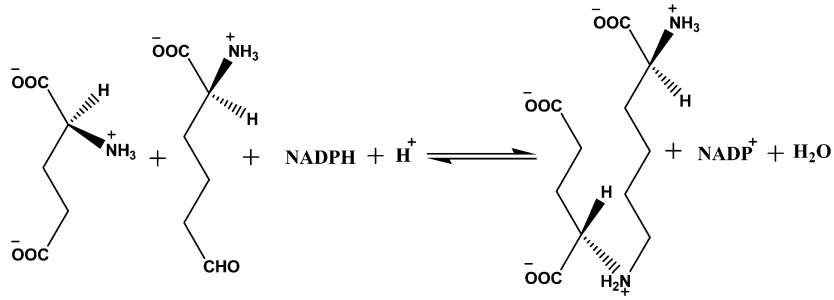

for SR. This is the first report of the kinetic mechanism of a saccharopine reductase.

MATERIALS AND METHODS

Chemicals. L-Saccharopine, L-pipecolic acid, glyoxylic acid, ornithine, L-glutamic acid, L-lysine, L-leucine, α-ketoglutarate, oxaloacetate, 5-bromopentene, ethylacetamidocyanoacetate, sodium metal, and chloramphenicol were from Sigma. β-NADPH, β-NADP, and LB broth were purchased from USB. The Ni-NTA agarose affinity resin was from Qiagen. Isopropyl β-D-1-thiogalactopyranoside was from Invitrogen, while ampicillin was from Fisher Biotechnologies, and ethanol-d_6 (99 atom % D) was purchased from Cambridge Isotope Laboratories, Inc. AG MP-1 and Bio-Gel P-2 resins were from Bio-Rad, and HEPES was obtained from Research Organics. *N*-Oxalylglycine was from Frontier Scientific. All chemicals were of the highest grade available and were used as purchased.

Synthesis of α*-Aminoadipic Acid* δ*-Semialdehyde.* The semialdehyde was synthesized using a modification of the method of Rodwell et al. (*13*). All of the equipment used for the synthesis was rinsed with acetone and dried overnight. To ethylacetamidocyanoacetate in ethanol was added sodium metal, and bromopentane was added dropwise over a period of 1 h. The mixture was refluxed for 1 h at 75 °C. The mixture was cooled to room temperature, and the ethanol was removed *in vacuo* using a Buchi rotatory evaporator at 60 °C. One percent NaOH was added to the residue, the mixture was refluxed at 102 °C for 15 h and cooled, and the pH was adjusted to 1.8 using 12 N HCl, followed by concentration by rotatory evaporation at 90 °C. The residue was dissolved in a minimum amount of water, and the pH was adjusted to 5.0 with pyridine, followed by addition of absolute ethanol. The crude solution was rotatory evaporated, dissolved in a minimum amount of water, and recrystallized using activated charcoal in hot water to obtain the HCl salt of 2-amino-6-heptenoic acid. Ozonolysis of the 2-amino-6-heptenoic acid in water was then carried out using an OREC Model V5-0 ozonator. The resulting aldehyde solution was purged with N_2 to remove excess ozone in the mixture. NMR spectra were obtained on a Varian Mercury VX-300 MHz spectrometer with a Varian 4-nuclei autoswitchable PFG probe. ^{1}H NMR spectra were collected in D_2O using the PRESAT pulse sequence supplied by Varian, Inc. The spectra were collected with a sweep width of 4803.1 Hz, eight transients, and an acquisition time of 3.411 s and processed with 108K data points resulting in a 1.0 Hz digital resolution. Chemical shifts were assigned for all peaks and are as follows: δ 9.7 [s, 1H, C(6)-H], 3.6 [t, 1H, C(2)-H], 1.78 [m, 2H, C(3)-H_2], 1.64 [t, 2H, C(5)-H_2], and 1.38 [p, 2H, C(4)-H_2].

The percent yield of semialdehyde was 95% for the ozonolysis step on the basis of the concentration of semialdehyde measured using end point assay using SR and monitoring the change in absorbance of NADPH at 340 nm. A resonance for the hydrated form of the aldehyde was not observed, suggesting that it lies under one of the other resonances. The end-point assay exhibited a rapid utilization of 65% of the aldehyde followed by a much slower utilization of the remaining 35%. Thus, 35% of the semialdehyde is present in the hydrated (or diol) form and 65% in the aldehyde form. The α-amino group of the semialdehyde is protonated at pH 7.0, and none of the cyclic imine was observed. The overall yield based on the starting material was 15%.

Synthesis of A-Side NADPD. The A-side NADPD was prepared using the method described by Viola et al. (*14*). The reaction mixture contained 5.6 mM NADP, 2.8 mM ethanol-d_6, 100 units each of alcohol dehydrogenase (*Thermoanaerobacter brockii*), and yeast aldehyde dehydrogenase. The reaction was carried out in 10 mL of 6 mM Ches, pH 9.0, at 25 °C. The reaction was allowed to proceed overnight, and the formation of NADPD was monitored by following the absorbance at 340 nm. The pH was constantly adjusted using KOH since the pH drops as the reaction proceeds. The reaction was terminated on the following day by adding a few drops of $CHCl_3$ to the reaction mixture with shaking, followed by separation of the aqueous layer from the organic layer. The aqueous layer was adjusted to pH 10.0 with KOH and loaded onto an AG-MP column equilibrated with 0.2 M LiCl (pH 10.0); fractions were eluted using 0.5 M LiCl (pH 10.0). The ratio of absorbance at 260 and 340 nm was 2.4 $\pm$ 0.05 for the pooled NADPD fractions compared to a value of 2.15 $\pm$ 0.05 reported preveiously (*14*). The purified A-side NADPD was then concentrated using rotatory evaporation at 50 °C to about 6 mL, and the solution was loaded onto a Bio-Gel P-2 column equilibrated with 50 mM KH_2PO_4. The NADPD was eluted using the same buffers and used without further treatment.

Cell Growth, Expression, and Protein Purification. The gene from *S. cerevisiae* encoding for SR (*LYS9*) was cloned into the pET-16b vector (*12*). The vector containing the insert was transformed into BL21*(DE-3) RIL *Escherichia coli* cells using heat shock at 42 °C, followed by growth on ampicillin plates. Colonies were picked, and cells were grown overnight at 37 °C in LB media containing 100 μg/mL ampicillin and 25 μg/mL chloramphenicol. The cells were induced using 1 mM IPTG at an A_{600} of 0.7−0.9 and allowed to grow overnight. After centrifugation at 4000*g*, the harvested cells were suspended in 100 mM Tris-HCl, pH 7.5, with 300 mM KCl.

For protein purification, PMSF (1 mM) was added to the cell suspension followed by cell disruption using a MISONIX sonicator XL. Sonication was carried out on ice for 1 min using a pulse-on time of 15 s followed by a 30 s rest period. The cell debris was removed by centrifugation at 20400*g* for 15 min, and the supernatant was loaded onto a Ni-NTA column, washed with 30 mM imidazole, and then eluted using buffer containing 400 mM imidazole at pH 7.5. The enzyme elutes efficiently using 400 mM imidazole and is about 98% pure on the basis of SDS−PAGE.

Enzyme Assay. The SR reaction was followed by monitoring the appearance or disappearance of NADPH at 340 nm (ϵ_{340}, 6220 M^{-1} cm^{-1}) using a Beckman DU-640 spectrophotometer. All assays were carried out at 25 °C. A typical assay in 500 μL contained 100 mM HEPES, pH 7.0, and appropriate concentrations of substrates. Reaction was initiated by adding 10 μL of appropriately diluted enzyme in 100 mM HEPES, pH 7.0. All enzyme dilutions were made fresh for each set of experiments.

Initial Velocity Studies. Studies were carried out in the forward and reverse reaction direction at pH 7.0. The rate of reaction in the direction of saccharopine formation was measured as a function of the concentration of NADPH (5−50 μM), at different fixed concentrations of L-glutamate (5−50 mM), and a fixed concentration of L-AASA (5 mM). The experiment was then repeated at different concentrations of AASA (7.14−12.5 mM). In the direction of AASA formation, initial rate data were collected as a function of NADP (0.02−0.5 mM) at different fixed saccharopine concentrations (0.1−10 mM).

Inhibition Studies. Product inhibition studies were carried out by measuring the initial velocity with fixed substrates equal to their respective K_m values and varying the concentration of the other substrate around its K_m value (0.5−5 K_m) at different fixed concentrations of the inhibitor including zero. First, an estimate of the inhibition constant of an inhibitor was obtained by measuring the initial rate as a function of the inhibitor concentration with all substrates fixed at their respective K_m values. The apparent K_i was then calculated from a plot of $1/v$ vs I with the apparent K_i value equal to the abscissa intercept divided by 2.

Primary Substrate Deuterium Kinetic Isotope Effects. Isotope effects were measured using NADPD as the deuterated substrate. $^{D}V_1$ and $^{D}(V_1/K_{glutamate})$ were obtained by measuring the initial rate as a function of L-glutamate concentration with NADPH(D) and α-AASA maintained at $10K_m$ and $5K_m$, respectively. Similarly, $^{D}(V_1/K_{NADPH})$ was obtained by varying NADPH(D) with glutamate and AASA fixed at saturation. All isotope effects were measured in triplicate, and the SEM is reported.

Data Processing. All data were plotted in double reciprocal form to assess the quality of the data and to determine the correct rate equation for data fitting. Initial velocity data were then fitted to the appropriate equation using the Enzfitter program from BIOSOFT, Cambridge, U.K. Initial velocity data in the direction of saccharopine formation were fitted to eqs 1 and 2, while data in the direction of AASA formation were fitted to eq 3. Data adhering to linear competitive, uncompetitive, and noncompetitive inhibition were fitted to eqs 4−6.

$$v = V_1ABC/\text{constant} + (\text{coef } A)A + (\text{coef } B)B + (\text{coef } C)C + K_cAB + K_bAC + K_aBC + ABC \quad (1)$$

$$v = \frac{V_1ABC}{K_{ia}K_{ib}K_c + K_{ib}K_cA + K_cAB + K_aBC + ABC} \quad (2)$$

$$v = \frac{V_2AB}{K_{ia}K_b + K_bA + K_aB + AB} \quad (3)$$

$$v = \frac{\text{app } VA}{K_a\left(1 + \frac{I}{K_{is}}\right) + A} \quad (4)$$

$$v = \frac{\text{app } VA}{K_a + A\left(1 + \frac{I}{K_{ii}}\right)} \quad (5)$$

$$v = \frac{\text{app } VA}{K_a\left(1 + \frac{I}{K_{is}}\right) + A\left(1 + \frac{I}{K_{ii}}\right)} \quad (6)$$

In eqs 1−6, v represents the measured initial velocity, app V is the maximum rate, obtained with fixed substrate equal to K_m, V_1 and V_2 are the maximum rates in forward and reverse reaction directions, A, B, and C are substrate concentrations, K_a, K_b, and K_c are Michaelis constants for substrates A, B, and C, respectively, I is the inhibitor concentration, K_{ia} and K_{ib} are the dissociation constants for EA and EB complexes, and K_{ii} and K_{is} are the intercept and slope inhibition constants, respectively. In eq 1, the constant and coefficient terms are products of kinetic constants and are mechanism dependent.

Direct Determination of K_{eq}. In order to determine the equilibrium constant, the concentrations of saccharopine, L-AASA, NADP, and NADPH were fixed at 1, 5, 0.5, and 0.1 mM, respectively, and the concentration of L-glutamate was varied in separate reactions from 0.2 to 8 mM at pH 7.0. Sufficient enzyme was added to each reaction mixture to bring the reaction rapidly to equilibrium. The absorbance was recorded before and after adding the enzyme, and a plot of ΔAbs vs glutamate was constructed. The concentration of L-glutamate that gave ΔAbs of zero was then used to calculate K_{eq} using eq 7.

$$K_{eq} = \frac{[\text{NADP}][\text{saccharopine}]}{[\text{NADPH}][\text{L-glutamate}][\text{AASA}]} \quad (7)$$

RESULTS

Initial Velocity Studies. In the direction of saccharopine formation, the double reciprocal plots obtained as described in Materials and Methods all intersect to the left of the ordinate. A fit of the data to eq 1 indicated the coef B, coef C, and K_b terms were indeterminate. Data were then fitted to eq 2, which suggest a kinetic mechanism with ordered addition of A followed by rapid equilibrium addition of B, followed by addition of C. Values of kinetic parameters are given in Table 1. Initial velocity patterns were also generated in the direction of semialdehyde formation by varying the concentration of saccharopine at different fixed concentrations of NADP. An intersecting pattern was obtained. The data were fitted to eq 3, and estimates of kinetic parameters are summarized in Table 1.

Product Inhibition Studies. In order to obtain additional quantitative information on the kinetic mechanism and test

Table 1: Summary of Kinetic Parameters for SR at pH 7.0

forward reaction		reverse reaction	
V_1/E_t (s^{-1})	8 ± 1	V_2/E_t (s^{-1})	1.06 ± 0.02
$V_1/K_{NADPH}E_t$ (M^{-1} s^{-1})	$(7.3 \pm 1.8) \times 10^5$	$V_2/K_{NADP}E_t$ (M^{-1} s^{-1})	$(5.67 \pm 0.01) \times 10^3$
$V_1/K_{Glu}E_t$ (M^{-1} s^{-1})	$(2.9 \pm 0.7) \times 10^2$	$V_2/K_{Sacc}E_t$ (M^{-1} s^{-1})	$(1.6 \pm 0.3) \times 10^2$
K_{NADPH} (μM)	11.4 ± 2.6	K_{NADP} (mM)	0.187 ± 0.006
K_{Glu} (mM)	28 ± 6	K_{Sacc} (mM)	6.6 ± 0.2
K_{iAASA} (mM)	4.4 ± 1.7	K_{iNADP} (mM)	0.020 ± 0.004
K_{iNADPH} (μM)	4.4 ± 2.1		

Table 2: Summary of Product Inhibition Data for Saccharopine Reductase

varied substrate	fixed substrate	inhibitor	K_{is} (mM)	K_{ii} (mM)	inhibition pattern	
					observed	predicted[a]
NADPH	L-glutamate (K_m),[b] L-AASA ($2K_{ib}$)	NADP	0.015 ± 0.002	N/A	C	C
L-AASA	NADPH (K_m), L-glutamate (K_m)	NADP	0.055 ± 0.012	0.042 ± 0.004	NC	NC
L-glutamate	NADPH (K_m), L-AASA ($2K_{ib}$)	NADP	0.038 ± 0.004	0.09 ± 0.01	NC	NC
NADPH	L-glutamate (K_m), L-AASA ($2K_{ib}$)	saccharopine	2.0 ± 0.4	1.6 ± 0.1	NC	NC
L-AASA	NADPH (K_m), L-glutamate (K_m)	saccharopine	0.55 ± 0.07	22 ± 12	NC	NC
L-glutamate	NADPH (K_m), L-AASA ($2K_{ib}$)	saccharopine	1.9 ± 0.3	1.00 ± 0.07	NC	NC
NADP	saccharopine (K_m)	NADPH	0.07 ± 0.01	N/A	C	C
saccharopine	NADP (K_m)	NADPH	0.008 ± 0.001	0.020 ± 0.003	NC	NC
NADP	saccharopine (K_m)	L-glutamic acid	0.14 ± 0.01	139 ± 10	NC	NC
saccharopine	NADP (K_m)	L-glutamic acid	5.7 ± 0.2	86 ± 10	NC	NC
NADP	saccharopine (K_m)	L-AASA			UC	UC
saccharopine	NADP (K_m)	L-AASA[c]			NC	UC

[a] Patterns predicted for an ordered kinetic mechanism. [b] Concentration of the fixed substrate. [c] AASA shows weak inhibition. Qualitatively, the inhibition pattern for AASA vs saccharopine is noncompetitive, suggesting that there may be some randomness in addition of AASA and glutamate.

Table 3: Summary of Dead-End Inhibition Data for SR

varied substrate	fixed substrate	inhibitor	K_{is} (mM)[a]	K_{ii} (mM)[a]	inhibition pattern		enzyme form[b]
					observed	predicted	
NADPH	L-glutamate (K_m), L-AASA ($2K_{ib}$)	α-Kg	N/A	7.0 ± 0.4 (1.4 ± 0.1)	UC	UC	E−NADPH−AASA
L-AASA	NADPH (K_m), L-glutamate (K_m)	α-Kg	N/A	9.4 ± 0.5 (4.6 ± 0.2)	UC	UC	E−NADPH−AASA
L-glutamate	NADPH (K_m), L-AASA ($2K_{ib}$)	α-Kg	8.2 ± 0.4 (4.0 ± 0.3)	N/A	C	C	E−NADPH−AASA
NADPH	L-glutamate (K_m), L-AASA ($2K_{ib}$)	aminoheptenoic acid	N/A	336 ± 41 (67 ± 8)	UC	UC	E−NADPH
L-AASA	NADPH (K_m), L-glutamate (K_m)	aminoheptenoic acid	65 ± 7 (47 ± 5)	N/A	C	C	E−NADPH
L-glutamate	NADPH (K_m), L-AASA ($2K_{ib}$)	aminoheptenoic acid	325 ± 134 (96 ± 38)	250 ± 36 (50 ± 7)	NC	NC	E−NADPH
NADP	saccharopine (K_m)	NOG	N/A	10.0 ± 0.4 (5.0 ± 0.2)	UC	UC	E−NADP
saccharopine	NADP (K_m)	NOG	7.0 ± 0.8 (6.0 ± 0.7)	N/A	C	C	E−NADP
NADP	saccharopine (K_m)	L-pipecolic acid	N/A	87 ± 6 (43 ± 3)	UC	UC	E−NADP
saccharopine	NADP (K_m)	L-pipecolic acid	38 ± 7 (34 ± 6)	N/A	C	C	E−NADP
NADP	saccharopine (K_m)	L-leucine	N/A	38 ± 2 (19 ± 1)	UC	UC	E−NADP
saccharopine	NADP (K_m)	L-leucine	17 ± 2 (15 ± 2)	N/A	C	C	E−NADP
NADP	saccharopine (K_m)	α-Kg	N/A	14.4 ± 0.5 (7.0 ± 0.3)	UC	UC	E−NADP
saccharopine	NADP (K_m)	α-Kg	11.1 ± 0.6 (10.0 ± 0.5)	N/A	C	C	E−NADP
NADP	saccharopine (K_m)	glyoxylic acid	N/A	14.2 ± 0.7 (7.0 ± 0.4)	UC	UC	E−NADP
saccharopine	NADP (K_m)	glyoxylic acid	8.7 ± 0.6 (8.0 ± 0.6)	N/A	C	C	E−NADP
NADP	saccharopine (K_m)	L-ornithine	N/A	13.7 ± 0.4 (7.0 ± 0.2)	UC	UC	E−NADP
saccharopine	NADP (K_m)	L-ornithine	11.6 ± 1.2 (10 ± 1)	N/A	C	C	E−NADP

[a] The values in parentheses are the corrected values for the fixed substrate where applicable. [b] Enzyme form to which the inhibitor binds.

the mechanism proposed from initial velocity studies in the absence of inhibitors, product inhibition patterns were obtained for all products in both reaction directions. Product inhibition by NADPH vs NADP is competitive, consistent with addition of the oxidized and reduced cofactor to free enzyme. AASA is uncompetitive vs NADP and noncompetitive vs saccharopine. All other patterns are noncompetitive and are consistent with the proposed ordered mechanism (Table 2).

Dead-End Inhibition Studies. To further test the proposed kinetic mechanism and obtain information on the reactant binding determinants, dead-end inhibition experiments were also carried out. All patterns are consistent with the ordered mechanism (Table 3).

Determination of K_{eq}. The equilibrium constant for the reaction catalyzed by saccharopine dehydrogenase was determined at pH 7.0 by determining the concentration of L-glutamate that gave no change in absorbance at fixed

concentration of all of the other substrates. The calculated K_{eq} value is 200 M^{-1}, in good agreement with 500 M^{-1}, the value determined using the Haldane relationship (eq 8).

$$K_{eq} = \frac{(V/K_{Glu})(K_{iNADP})}{(V/K_{Sacc})(K_{iNADPH})(K_{iAASA})} \quad (8)$$

Primary Substrate Deuterium Kinetic Isotope Effects. Isotope effect studies were carried out at pH 7.0 using A-side NADPD as the deuterated substrate. The isotope effects measured are all small: $^{D}V_1 = 1.2 \pm 0.1$, $^{D}(V_1/K_{glutamate}) = 0.870 \pm 0.035$, and $^{D}(V_1/K_{NADPH}) = 0.98 \pm 0.04$. Values of $^{D}V_1$ and $^{D}(V_1/K_{NADPH})$ are near unity, while the value of $^{D}(V_1/K_{glutamate})$ is inverse.

DISCUSSION

Initial Velocity Studies. In the direction of saccharopine formation, intersecting patterns were obtained using a fixed nonsaturating concentration of α-AASA and varying NADPH/L-glutamate. Intersecting patterns were also obtained in the direction of saccharopine oxidation. Data are consistent with a sequential mechanism.

The initial velocity data in the direction of saccharopine formation were obtained as a function of the concentration of NADPH (5−50 μM), at different fixed concentrations of L-glutamate (5−50 mM), and a fixed concentration of L-AASA (5 mM). This experiment was then repeated at different fixed concentrations of AASA and data were fitted to eq 1 for a fully random terreactant mechanism; the fitted parameters showed that coef *B*, coef *C*, and K_b terms in the denominator of eq 1 were not defined. Data suggest that the EB (E-AASA) and EC (E-L-glutamate) binary complexes are not present. The absence of the K_{AASA} term in eq 2 indicates that the binding of AASA must be in equilibrium, which suggests that it binds after NADPH and before glutamate. Data were then fitted to eq 2 for an ordered mechanism with AASA adding in rapid equilibrium, and all kinetic parameters were well defined (Table 1). On the basis of initial velocity studies in the absence of inhibitors, the mechanism is sequential with an apparent requirement for NADPH bound prior to AASA or glutamate. The maximum rate in the physiological reaction direction is 8 times higher than that in the nonphysiological reaction direction.

Product Inhibition Studies. Inhibition studies can be used to further define the kinetic mechanism of an enzyme-catalyzed reaction. They provide information regarding the various enzyme forms to which substrates bind and thus the order of addition of substrates. In the direction of saccharopine formation, product inhibition studies were carried out using NADP and saccharopine as product inhibitors. NADP is competitive vs NADPH and noncompetitive vs α-AASA and L-glutamate, while saccharopine exhibited noncompetitive inhibition against all three reactants, NADPH, α-AASA, and L-glutamate. In the direction of saccharopine oxidation, NADPH is competitive vs NADP and noncompetitive vs saccharopine. L-Glutamate exhibited noncompetitive inhibition vs both NADP and saccharopine, while α-AASA showed noncompetitive inhibition vs saccharopine and uncompetitive inhibition vs NADP. Data suggest that, in the direction of saccharopine formation, AASA binds to the E−NADPH binary complex in rapid equilibrium fashion followed by the addition of L-glutamate, while in the direction of saccharopine oxidation, NADP is the first substrate to be added followed by saccharopine, which adds to the E−NADP binary complex.

Dead-End Inhibition Studies. In the direction of saccharopine formation, dead-end inhibition patterns were obtained using analogues of L-glutamate and α-AASA. 2-Amino-6-heptenoic acid was competitive vs AASA, uncompetitive vs NADPH, and noncompetitive vs L-glutamate, showing that 2-amino-6-heptenoic acid (and by analogy AASA) binds to E−NADPH. α-Ketoglutarate was chosen as the dead-end analogue of L-glutamate and exhibited competitive inhibition vs L-glutamate and uncompetitive inhibition vs AASA and NADPH, consistent with binding of L-glutamate to the E−NADPH−AASA ternary complex. In the direction of oxidation of saccharopine, dead-end analogues of saccharopine are competitive vs saccharopine and uncompetitive vs NADP, in agreement with binding of the analogues to E−NADP. Product and dead-end inhibition data are consistent with an overall ordered kinetic mechanism for SR, as shown by the agreement between the observed inhibition patterns and those predicted for an ordered mechanism (Tables 2 and 3). The proposed mechanism is depicted in Scheme 1.

Calculation of True Dead-End Inhibition Constants. Inhibition constants obtained in product and dead-end inhibition studies are apparent values since the fixed substrate(s) is (are) present at a concentration equal to their K_m value. In the case of dead-end inhibitors, true inhibition constant values can be estimated by correcting for the presence of the fixed reactant. The true K_i value will thus be independent of the substrate varied, as long as it results from combination to the same enzyme form(s). The rate equation for the SR kinetic mechanism in the direction of saccharopine formation is given in eq 2. Each term in the denominator of eq 2 reflects an enzyme form. The $K_{ia}K_{ib}K_c$ and K_aBC terms represent free

Scheme 1: Proposed Kinetic Mechanism for SR[a]

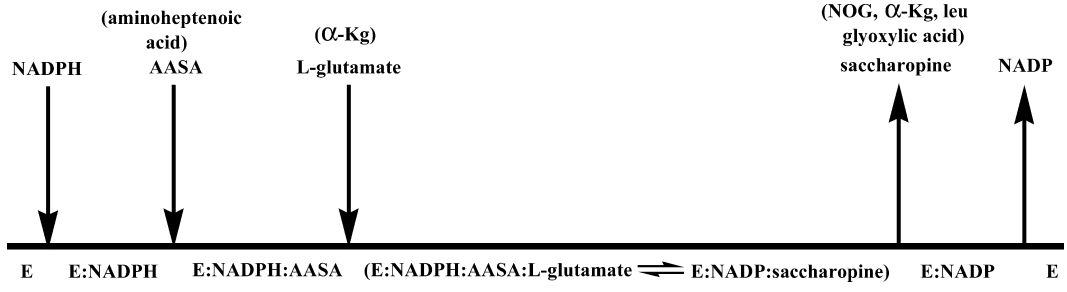

[a] Dead-end analogues of the substrates are shown in parentheses.

enzyme, while $K_{ib}K_cA$, K_cAB, and ABC terms represent the E−NADPH, E−NADPH−AASA, and the central and product complexes present at steady state, respectively.

The equation for correction of the apparent K_i values can easily be derived, and the overall strategy is illustrated by an example below. If a competitive dead-end inhibitor of substrate B (L-AASA in the terreactant direction) is used, the presence of the inhibitor modifies the enzyme form(s) to which B binds, i.e., the $K_{ib}K_cA$ term in eq 2, by a factor of $(1 + I/K_i)$ to give eq 9, where K_i is the intrinsic dissociation constant for the inhibitor.

$$v = \frac{VABC}{K_{ia}K_{ib}K_c + K_aBC + (K_{ib}K_c)\left(1 + \frac{I}{K_i}\right)A + K_cAB + ABC} \quad (9)$$

The double reciprocal form factoring out (1/*B*) gives eq 10

$$\frac{1}{v} = \left[\left(\frac{K_{ia}K_{ib}K_c}{VAC} + \frac{K_{ib}K_c}{VC}\right) + \left(\frac{K_{ib}K_c}{VC}\right)\left(\frac{I}{K_i}\right)\right]\left(\frac{1}{B}\right) + \left(\frac{K_a}{VA} + \frac{K_c}{VC} + \frac{1}{V}\right) \quad (10)$$

The expression for the slope term in eq 10 is given by eq 11.

$$\text{slope} = \left(\frac{K_{ia}K_{ib}K_c}{VAC} + \frac{K_{ib}K_c}{VC}\right) + \left(\frac{K_{ib}K_c}{VK_iC}\right)I \quad (11)$$

Setting the slope equal to zero and solving for I (app K_i) gives eq 12.

$$\text{app } K_i = -K_i\left(1 + \frac{K_{ia}}{A}\right) \quad (12)$$

Thus, the intrinsic K_i is calculated using known values of app K_i, K_{ia}, and A. A similar treatment gives eq 13 when 1/*A* is factored out of eq 10.

$$\frac{1}{v} = \left(\frac{K_{ia}K_{ib}K_c}{VBC} + \frac{K_a}{V}\right)\left(\frac{1}{A}\right) + \frac{K_{ib}K_c}{VBC}\left(1 + \frac{I}{K_i}\right) + \frac{K_c}{VC} + \frac{1}{V} \quad (13)$$

$$\text{app } K_{ii} = K_i\left[1 + \left(\frac{B}{K_{ib}}\right)\left(1 + \frac{C}{K_c}\right)\right] \quad (14)$$

Using this kind of analysis, estimates of intrinsic K_i values are calculated, and these are shown in parentheses in Table 3. Binding of a dead-end analogue to a given enzyme form, whatever substrate is varied, should give the same K_i when the apparent K_i is corrected for the presence of the fixed reactant(s). The agreement in the intrinsic K_i values for dead-end analogues estimated under different conditions is consistent with the proposed ordered mechanism.

Primary Kinetic Deuterium Isotope Effects. The values of primary deuterium isotope effects obtained by direct comparison of *V* and *V/K* values in the direction of formation of saccharopine are small, suggesting that the hydride transfer step is not slow in the overall reaction. In an ordered mechanism, the isotope effects on the *V/K* of all but the final substrate to add to the enzyme in either reaction direction is unity. In agreement with the proposed ordered mechanism, $^D(V/K_{NADPH})$ is within error 1. The inverse isotope effect observed for $^D(V/K_{glutamate})$ suggests that the hydride transfer step is close to equilibrium in the steady state. The equilibrium isotope effect for reduction of an imine reflects the difference in fractionation factor for deuterium at C4 of NADPD and C6 of saccharopine. The value of $^DK_{eq}$ was estimated as 0.87 from glutamate and alanine dehydrogenases (*16*), and this is equal to $^D(V/K_{glutamate})$. Thus, (a) step(s) after reduction of the imine limit(s) the overall reaction, likely the conformational change to open the active site to release saccharopine. Data further suggest the deuterium isotope effect on *V* is unity and not a small finite value, since a finite isotope effect other than unity should be inverse as observed for $^D(V/K_{glutamate})$.

Comparison of the Kinetic Mechanism of SR with Similar Enzymes. Enzymes that catalyze the pyridine nucleotide dependent oxidative deamination of an amino acid fall into two classes, those that function with primary amines and those that function with secondary amines. The best studied examples of the primary amine dehydrogenases are glutamate (*15*−*19*) and alanine (*16, 20, 21*) dehydrogenases, while saccharopine dehydrogenase is the only secondary amine dehydrogenase (*22*−*24*) that was characterized with respect to its kinetic mechanism prior to this study.

The primary amine dehydrogenases catalyze a reversible oxidative deamination of an amino acid to give ammonia and an α-keto acid with NAD(P) serving as the oxidant. The kinetic mechanism of glutamate dehydrogenase (GDH) from bovine liver has been best studied and has a random kinetic mechanism on the basis of steady-state and pre-steady-state studies and isotope effects (*15*−*19*). On the other hand, the kinetic mechanism of alanine dehydrogenase from thermophilic *Bacillus sphaericus*, and *Bacillus subtilis*, is ordered (*20, 21*).

Kinetic mechanisms of other amine dehydrogenases have also been reported. Leucine dehydrogenase from *Natronobacterium magaddi* (*25*), a halophilic thermophile, *Bacillus licheniformis* TSN9 (*26*), and *Bacillus stearothermophilus* (*27*) also have a sequential ordered kinetic mechanism. Phenylalanine dehydrogenase from *Thermoactinomyces* (*28*), *Rhodococcus maris* (*29*), and *Rhodococcus* sp. (*30*), diaminopimelate dehydrogenase from *B. sphaericus* (*31*), and valine dehydrogenase (which is specific for branched chain amino acid substrates) from *Streptomyces cinnamonensis* (*32*) all show a sequential ordered mechanism, with the exception of the valine dehydrogenase from *Alcaligenes faecalis* (*33*), which apparently has a random mechanism. Thus, although most of the enzymes from this class exhibit an ordered mechanism, there is no consensus.

The kinetic mechanism of saccharopine dehydrogenase (L-lysine forming) from *S. cerevisiae* catalyzes the final step in the lysine biosynthetic pathway in yeast and catalyzes the reversible oxidative deamination of saccharopine to generate α-Kg and lysine using NAD as an oxidant (*1*). The last two enzymes in the pathway, saccharopine reductase and saccharopine dehydrogenase, bind the same substrate, saccharopine, and catalyze oxidation of adjacent bonds in the secondary amine. SR and SDH have little or no similarity in their primary, secondary, and tertiary structure, with the exception of the Rossman fold which binds the dinucleotide (*10, 34*). The kinetic mechanism of the two enzymes is very similar, with ordered addition of NAD(P) and saccharopine and release of the reduced dinucleotide last. The addition of L-AASA and glutamate is ordered in the case of SR, while

addition of α-Kg and lysine is random for SDH (refs (*22*) and (*24*) and this study).

REFERENCES

1. Xu, H., Andi, B., Qian, J., West, A. H., and Cook, P. F. (2006) The α-aminoadipate pathway for lysine biosynthesis in fungi. *Cell Biochem. Biophys. 46*, 43–64.
2. Nishida, H., Nishiyama, M., Kobashi, N., Kosuge, T., Hoshino, T., and Yamane, H. (1999) A prokaryotic gene cluster involved in synthesis of lysine through the aminoadipate pathway: A key to the evolution of amino acid biosynthesis. *Genome Res. 9*, 1175–1183.
3. Broquist, H. P. (1971) Lysine biosynthesis (yeast). *Methods Enzymol. 17*, 112–129.
4. Ye, Z. H., and Bhattacharjee, J. K. (1988) Lysine biosynthesis pathway and biochemical blocks of lysine auxotrophs of *Schizosaccharomyces pombe*. *J. Bacteriol. 170*, 5968–5970.
5. Jaklitsch, W. M., and Kubicek, C. P. (1990) Homocitrate synthase from *Penicillium chrysogenum*. Localization, purification of the cytosolic isoenzyme, and sensitivity to lysine. *J. Biochem. 269*, 247–253.
6. Trupin, J. S., and Broquist, H. P. (1965) Saccharopine, an intermediate of the aminoadipic acid pathway of lysine biosynthesis. I. Studies in *Neurospora crassa*. *J. Biol. Chem. 240*, 2524–2530.
7. Johansson, E., Steffens, J. J., Lindqvist, Y., and Schneider, G. (2000) Crystal structure of saccharopine reductase from *Magnaporthe grisea*, an enzyme of the α-aminoadipate pathway of lysine biosynthesis. *Structure 8*, 1037–1047.
8. Garrad, R. C., and Bhattacharjee, J. K. (1992) Lysine biosynthesis in selected pathogenic fungi: characterization of lysine auxotrophs and the cloned *LYS1* gene of *Candida albicans*. *J. Bacteriol. 174*, 7379–7384.
9. Palmer, D. R., Balogh, H., Ma, G., Zhou, X., Marko, M., and Kaminskyj, S. G. (2004) Synthesis and antifungal properties of compounds which target the alpha-aminoadipate pathway. *Pharmazie 59*, 93–98.
10. Andi, B., Cook, P. F., and West, A. H. (2006) Crystal structure of his-tagged saccharopine reductase from *Saccharomyces cereviciae* at 1.7Å resolution. *Arch. Biochem. Biophys. 46*, 243–254.
11. Storts, D. R., and Bhattacharjee, J. K. (1987) Purification and properties of saccharopine dehydrogenase (glutamate forming) in *Saccharomyces cerevisiae* lysine biosynthetic pathway. *J. Bacteriol. 169*, 416–418.
12. Jones, E. E., and Broquist, H. P. (1966) Saccharopine, an intermediate of the aminoadipic acid pathway of lysine biosynthesis. III. Aminoadipic semialdehyde-glutamate reductase. *J. Biol. Chem. 241*, 3430–3434.
13. Rodwell, V. W. (1971) δ-1-Piperdine-6-carboxylic acid and α-aminoadipic acid δ-semialdehyde. *Methods Enzymol. 17*, 188–199.
14. Viola, R. E., Cook, P. F., and Cleland, W. W. (1979) Stereoselective preparation of deuterated reduced nicotinamide adenine nucleotides and substrates by enzymatic synthesis. *Anal. Biochem. 96*, 334–340.
15. Cook, P. F. (1982) Kinetic studies to determine the mechanism of regulation of bovine liver glutamate dehydrogense by nucleotide effectors. *Biochemistry 21*, 113–116.
16. Weiss, P. M., Chen, C. Y., Cleland, W. W., and Cook, P. F. (1988) Use of primary deuterium and ^{15}N isotope effects to deduce the relative rates of steps in the mechanisms of alanine and glutamate dehydrognases. *Biochemistry 27*, 4814–4822.
17. Frieden, C. F. (1959) Glutamic dehydrogenase. The order of substrate addition in the enzymatic reaction. *J. Biol. Chem. 234*, 2891–2896.
18. Engel, P. C., and Dalziel, K. (1970) Kinetic studies of glutamate dehydrogenase. The reductive amination of 2-oxoglutarate. *Biochem. J. 118*, 409–419.
19. Colen, A. H., Prough, R. A., and Fisher, H. F. (1972) The mechanism of the glutamate dehydrogenase reaction. Evidence for random and rapid binding of substrate and coenzyme in the burst phase. *J. Biol. Chem. 247*, 7905–7909.
20. Ohshima, T., Sakane, M., Yamazaki, T., and Soda, K. (1990) Thermostable alanine dehydrogenase from thermophilic *Bacillus sphaericus* DSM 462. Purification, characterization and kinetic mechanism. *Eur. J. Biochem. 191*, 715–720.
21. Grimshaw, C. E., and Cleland, W. W. (1981) Kinetic mechanism of *Bacillus subtilis* L-alanine dehydrogenase. *Biochemistry 20*, 5650–5655.
22. Fujioka, M., and Nakatani, Y. (1970) A kinetic study of the saccharopine dehydrogenase reaction. *Eur. J. Biochem. 16*, 180–186.
23. Fujioka, M., and Nakatani, Y. (1972) Saccharopine dehydrogenase, interaction with substrate analogues. *Eur. J. Biochem. 25*, 301–307.
24. Xu, H., West, A. H., and Cook, P. F. (2006) Overall kinetic mechanism of saccharopine dehydrogenase from *Saccharomyces cerevisiae*. *Biochemistry 45*, 12156–12166.
25. Katoh, R., Ngata, S., Ozawa, A., Ohshima, T., Kamekura, M., and Misono, H. (2003) Purification and characterization of leucine dehydrogenase from an alkaliphilic halophile *Natronobacterium magadii* MS-3. *J. Mol. Catal. B: Enzym. 23*, 231–238.
26. Nagata, S., Bakthavatsalam, S., Galkin, A. G., Asada, H., Sakai, S., Esaki, N., Soda, K., Ohshima, T., Nagasaki, S., and Misono, H. (1995) Gene cloning, purification, and characterization of thermostable and halophilic leucine dehydrogenase from a halophilic thermophile, *Bacillus licheniformi* TSN9. *Appl. Microbiol. Biotechnol. 44*, 432–438.
27. Ohshima, T., Misono, H., and Soda, K. (1978) Properties of crystalline leucine dehydrogenase from *Bacillus sphaericus*. *J. Biol. Chem. 253*, 5719–5725.
28. Ohshima, T., Takada, H., Yoshimura, T., Esaki, N., and Soda, K. (1991) Distribution, purification, and characterization of thermostable phenylalanine dehydrogenase from *Thermophilic actinomycetes*. *J. Bacteriol. 173*, 3943–3948.
29. Misono, H., Yonezawa, J., Nagata, S., and Nagasaki, S. (1989) Purification and characterization of a dimeric phenylalanine dehydrogenase from *Rhodococcus maris* K-18. *J. Bacteriol. 171*, 30–36.
30. Brunhuber, N. M. W, Thoden, J. B., Blanchard, J. S., and Vanhooke, J. L. (2000) *Rhodococcus* L-phenylalanine dehydrogenase: kinetics, mechanism, and structural basis for catalytic specifity. *Biochemistry 39*, 9174–9187.
31. Misono, H., and Soda, K. (1980) Properties of *meso*-α,ϵ-diaminopimelate D-dehydrogenase from *Bacillus sphaericus*. *J. Biol. Chem. 255*, 10599–10605.
32. Priestley, N. D., and Robinson, J. A. (1989) Purification and catalytic properties of L-valine dehydrogenase from *Streptomyces cinnamonensis*. *Biochem. J. 261*, 853–861.
33. Ohshima, T., and Soda, K. (1993) Valine dehydrogenase from a non-spore-forming bacterium, *Alcaligenes faecalis*: purification and characterization. *Biochim. Biophys. Acta 1162*, 221–226.
34. Andi, B., Xu, H., Cook, P. F., and West, A. H. (2007) Crystal structures of ligand-bound saccharopine dehydrogenase from *Saccharomyces cerevisiae*. *Biochemistry 46*, 12512–12521.

BI800086G